Journal of Applied Polymer Science

Selective Recognition of Beta-Cypermethrin by Molecularly Imprinted Polymers Based on Magnetite Yeast Composites

Wei-Sheng Guan, Jun-Ru Lei, Xu Wang, Ya Zhou, Chen-Chen Lu, Shao-Fang Sun
Ministry of Education, College of the Environmental Science and Engineering, Chang'an University, Xi'an 710054, People's Republic of China
Correspondence to: W.-S. Guan (E-mail: 570235114@qq.com)

ABSTRACT: Magnetic nanoparticles were attached to yeast by co-precipitation reaction of $FeCl_3 \cdot 6H_2O$ and $FeCl_2 \cdot 4H_2O$. Then, based on magnetite yeast composites (M@Y), the magnetic molecularly imprinted polymers (MMIPs) were synthesized for the selective recognition of beta-cypermethrin (PP_{321}). MMIPs were characterized by scanning electron microscopy, X-ray diffraction, vibrating sample magnetometer, Fourier transform infrared analysis, thermogravimetric analysis, and elemental analysis. MMIPs exhibited uniform morphology and magnetic property (Ms = 17.87 emu/g) and thermal stability. Batch mode adsorption studies were carried out to investigate the specific adsorption equilibrium, kinetics, and selective recognition. The Langmuir isotherm model was fitted to the equilibrium data slightly better than the Freundlich model, and the adsorption capacity of MMIPs was 39.64 mg/g at 298 K. The kinetic properties of MMIPs were well described by the pseudo-second-order equation. Hydrogen bonds between methacrylic acid and PP_{321} were mainly responsible for the adsorption mechanism. The MMIPs prepared were applied to the separation of PP_{321} from experimental samples successfully. © 2013 Wiley Periodicals, Inc. J. Appl. Polym. Sci. 129: 1952–1958, 2013

KEYWORDS: biosynthesis of polymers; molecular recognition; kinetics

Received 5 September 2012; accepted 29 November 2012; published online 3 January 2013
DOI: 10.1002/app.38879

INTRODUCTION

Pyrethroid pesticides (PPs) are increasingly used in agriculture, domestic, veterinary industry[1] attributed to their remarkable efficiency to pests, low toxicity to human beings,[2,3] as well as more stable properties, and have been listed in the environmental hormone by the United States. Discharge of PPs-contaminated wastewater into aquatic environment without appropriate treatment not only can pose many health disorders, but also cause negative effects on the water quality,[4] inducing the anxiolytic effect on pests.[5] Beta-cypermethrin (PP_{321}) has extensive application in many field and exist trace in aquatic environment. Solid phase extraction (SPE) as a commonly used technique to pretreat PP_{321}-contaminated wastewater,[6] owing to its simple operation, economic, and easy to recycle as well as decrease secondary pollution of organic solvent. However, poor thermal stability, nonselection and low adsorption capacity of conventional sorbent limit the more extensive application of SPE. Therefore, it is essential to study a novel method to prepare superior performance sorbent.

Molecular imprinting technique is a well analytical and detached method based on specific recognition properties between the artificial antigen–antibody.[7] It is a simple and widely used technique for synthesizing molecularly imprinted polymers (MIPs). Surface molecular imprinting technique[8] has been proved to be superior to the molecular imprinting technique, it improve mass transfer, have high recognition and binding ability, and reduce permanent entrapment of the template.[9] In the current study, silica-based micro-/nano-materials,[10] titanium-based micro-/nano-materials,[11] metallicoxide,[12] carbon nanotubes[13] have been widely used in the surface molecular imprinting process as solid-support substrates.

The inorganic materials above as matrixes have advantages of specific intensity, special structure, and stable performance, but lack of preferable compatibility and the high degree of conjunction performance with imprinting polymer layer. Thus, the great priority is given to the potential substitute for inorganic matrixes. Researchers have introduced microorganism as biosorbent.[14–16] Yeast are widely obtainable, much cheaper, free from pollution to the environment, possessing of large specific surface area and abundant functional groups such as carbonyls, amines, hydroxyls and phosphoryl,[17] inducing high compatibility with the organic polymer even metal ions. Then MIPs achieved have more recognition sites, efficient mechanical properties, binding affinity and adsorption stability.

Herein, magnetic solid support substrates show the advantage to be easily removed from the medium by a simple magnetic

© 2013 Wiley Periodicals, Inc.

separation and can utilize circularly, so it is better to combine yeast with magnetite (Fe_3O_4) to produce magnetic sorbent. Fe_3O_4 has ferromagnetic properties and effective binding to biomolecules,[18] one of the most popular magnetic materials used in various applications. In this study, we report an effective method to achieve magnetite@yeast composites (M@Y) as solid support substrates. Then M@Y were coated with a thin MIPs film, PP_{321} act as the target molecule in the film. Finally, the resultant magnetic molecularly imprinted polymers (MMIPs) could be the sorbent in simulative water samples and adsorb PP_{321} efficiently.

EXPERIMENTAL

Reagents and Materials

Yeast powder was provided by Angel Yeast Co., Ltd. Iron chloride tetrahydrate ($FeCl_2{\cdot}4H_2O$), ∂-methacrylic acid (∂-MAA), oleic acid, and methyl alcohol were obtained from Fuchen Chemical Reagent Factory (Tianjin, China). Sodium hydroxide and polyvinylpyrrolidone (PVP) were supplied by Paini Chemical Reagent Factory (Zhenzhou, China). Ferric chloride ($FeCl_3{\cdot}6H_2O$) (Tianjin Yaohua Chemical Co., China), Ammonia solution (Sichuan Xilong Chemical Co., China), dimethyl sulfoxide (DMSO, Guangdong Guanghua Sci-Tech Co., China), ethyleneglycol dimethacrylate (EGDMA, Aladdin Chemical Co., China), azobisisobutyronitrile (AIBN, Shanghai Shanpu Chemical Co., China), PP_{321}, beta-cyfluthrin. Except that AIBN was chemical grade and the purity of PP_{321} and beta-cyfluthrin was 95%, all the reagents were analytical grade. Distilled water was purchased from Xi'an.

Equipment

The morphology of MMIPs was observed by a scanning electron microscope (SEM, S-4800). The identification of crystalline phase was performed using a Rigaku D/max-γB X-ray diffraction (XRD) with monochromatized Cu Kαradiation over the 2θ range of 20–70° at a scanning rate of 0.02 °/s. Magnetic measurements were carried out using a vibrating sample magnetometer (7300, Lakeshore) under a magnetic field up to 15 k Oe. Fourier transform infrared spectra (FT-IR) were recorded on a Nicolet NEXUS-470 FT-IR apparatus. Thermogravimetric analysis (TGA) was performed for powder samples (about 5.0 mg) using a NETZSCH STA 449 C Instruments under a nitrogen atmosphere up to 800°C with a heating rate of 10.0 °C/min. Vario EL elemental analyzer (Elementar, Hanau, Germany) was employed to investigate the surface elemental composition of the prepared composites.

Synthesis of Fe_3O_4/Yeast Magnetic Particles

The synthetic process of Fe_3O_4/yeast nanomagnetic particles was followed by co-precipitation method.[19] As follows: 1.00 g yeast powder of about 2.8×10^{10} yeast cells were washed with 0.9% NaCl aqueous solution for several times and then were dissolved in 35 mL distilled water, 1.35 g $FeCl_3{\cdot}6H_2O$ were added into distilled water. Next, the mixture was continuously magnetic stirred at room temperature for 3 h in a three-necked round-bottomed flask, and a stable suspension was obtained. Then, 0.99 g $FeCl_2{\cdot}4H_2O$ was dissolved in the suspension with vigorous stirring under nitrogen atmosphere. When the solution temperature was increased to 80°C, 1.00 g NaOH added into suspension under stirring after 20 min, the mixture was continuously magnetic stirred at 80°C for 2 h in total. NH_4OH (25%, w/w) was added drop by drop and the reaction was maintained for 30 min. The black mixture was obtained, aging at room temperature for 12 h. The black materials was separated by a Nd-Fe-B permanent magnet, and washed several times by distilled water and alcohol. Finally, the black Fe_3O_4/yeast magnetic particles were dried under vacuum at 70°C.

Synthesis of PP_{321} Imprinted M@Y (MMIP)

The MMIPs were prepared following the literature[20] with the optimal synthesis conditions. The PP_{321} (450 mg) and MAA (345 μL) were dispersed into DMSO (10 mL) in an ultrasonic bath for 1 h at 25°C to obtain the preassembly solution. The M@Y (1.5 g) were mixed with oleic acid (4.0 mL) and oscillated in a three-necked round-bottomed flask for 10 min. Then EGDMA (4.0 mL) and the preassembly solution were added into the mixture of M@Y and oleic acid. This mixture was mechanically stirred for 30 min to obtain the prepolymerization solution. Moreover, the PVP (0.4 g) used as dispersant was dissolved into 100 mL of DMSO/water (9 : 1, v/v), added into the prepolymerization solution subsequently, and then AIBN (0.3 g) was also added into it slowly. The mixture was mechanical stirred under nitrogen while the temperature increased to 70°C. The reaction was allowed to proceed at 70°C for 24 h. After the polymerization, the mixture was washed with ethanol several times and the MMIPs were collected by an external magnetic field. Then, the obtained MMIPs were washed with the mixture solution of methanol/acetic acid (95 : 5, v/v) using Soxhlet extraction to remove the template molecules. Finally, the obtained MMIPs were dried at 70°C under vacuum. In comparison, the magnetic nonimprinted polymers (MNIPs) were also prepared as a blank in parallel but without the addition of PP_{321}.

Batch Mode Binding Studies

The experimental parameters such as pH, initial concentration of PP_{321}, temperature, and contact time on the adsorption of PP_{321} were studied in batch mode of operations. For this purpose, a certain amount of sorbent (MMIPs or MNIPs) was dispersed in testing solution of PP_{321} (10 mL). After the demanded time, the MMIPs and MNIPs were separated by an external magnetic field, and the concentration of PP_{321} in the solvent phase was determined with UV–vis 765 spectrophotometer (set wavelength at 278 nm for PP_{321}).

RESULTS AND DISCUSSION

Characterization of MMIPs and MNIPs

The morphology and structure of the obtained materials were investigated by SEM. As shown in Figure 1(a), the morphology of M@Y was approximately spherical with the diameters ranging from 2.5 to 3.2 μm. Obviously, yeast cells as templates were well treated with iron ions. Careful observation shows that the surfaces of these M@Y microspheres were constructed by many nanoparticles. The high-magnification SEM image in Figure 1(b) reveals the morphology of obtained MMIPs, which retain the morphology of the M@Y fairly well, but the dimension of particles and the roughness of the surface change considerably owing to the template molecule removed, with diameters

Applied Polymer SCIENCE

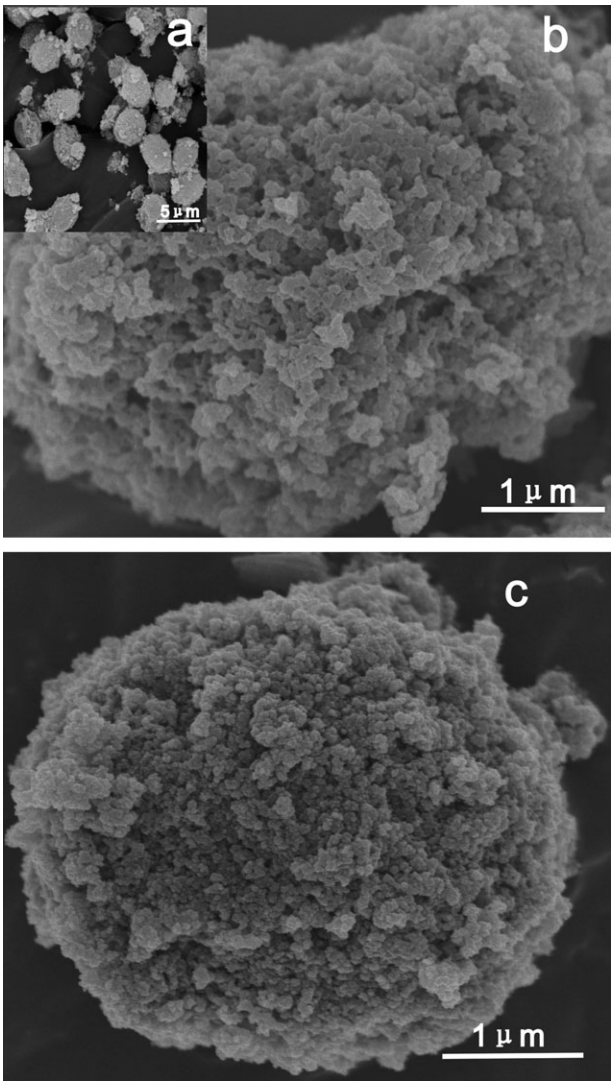

Figure 1. Micrographs from a SEM of M@Y(a), MMIPs (b), and MNIPs (c).

ranging from 3.5 to 4.3 μm. Figure 1(c) is the SEM image of the MNIPs microspheres. The obtained MNIPs microspheres were relatively uniform and the diameters between 3.2 and 4.0 μm. The slight increase in the size of MNIPs in comparison with M@Y provides assertive evidence that the film have wrapped the surface of the M@Y cores. Compared these samples, it can demonstrate that the thickness of the imprinted film for MMIPs and MNIPs were almost 1.0–1.1 and 0.7–0.8 μm, respectively.

Figure 2 shows the XRD patterns of M@Y (a), MMIPs (b), and MNIPs (c), in the 2θ range of 20°–70°, five characteristic peaks that corresponded to Fe_3O_4 (2θ = 30.19°, 35.27°, 43.29°, 57.15°, and 62.81°) were observed in the M@Y, MMIPs, and MNIPs. The peak positions could be indexed to (220), (311), (400), (511), and (440) (JCPDS card 19-0629 for Fe_3O_4). Moreover, it also can be seen that the XRD pattern of MNIPs and MNIPs were similar to that of M@Y, indicating they had the same cylinder wall structure and interplanar spacing. As shown in Figure 2, the three characteristic peaks of MMIPs mentioned above declined more than MNIPs owing to the encapsulation by the thicker polymer layer. The crystallite size could be estimated from broadening of the (311) peak by Scherrer formula:[21] From XRD results, the crystallite sizes on MMIPs and MNIPs were estimated to be about 39.8 and 15.5 nm, respectively.

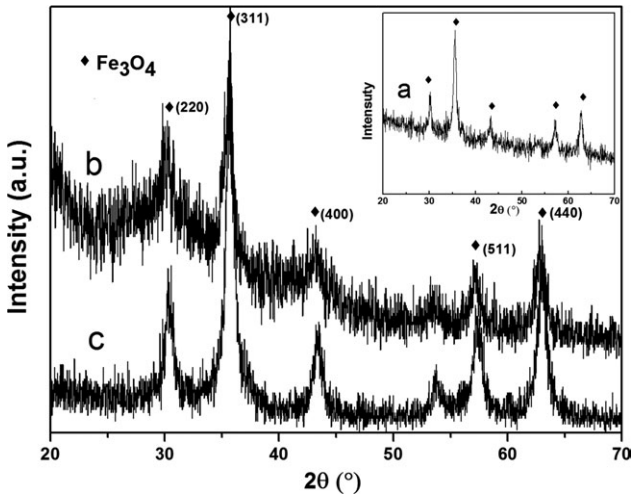

Figure 2. X-ray diffraction (XRD) patterns of M @Y (a), MMIPs (b), and MNIPs (c).

The magnetic hysteresis loop of MMIPs and MNIPs were showed in the Figure 3, respectively. It was obvious that there was a similar general shape and trend of the two curves in Figure 3(a), indicating two particles were superparamagnetic.[22] The saturation magnetization (Ms) values obtained at room temperature were 17.87 and 34.30 emu/g for MMIPs and MNIPs, respectively. The Ms value of MNIPs was greater than MMIPs for the thinner imprinted film of MNIPs. Even more, because of a magnetically inactive layer of nanoparticles that were not

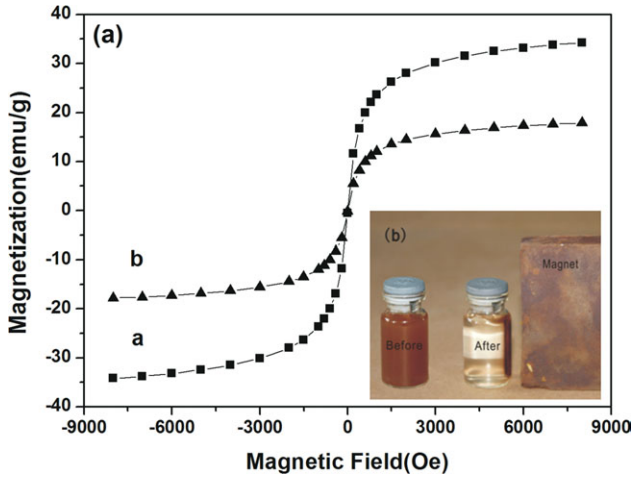

Figure 3. (a) Magnetization curves at 298 K of MMIPs (i), and MNIPs (ii). (b) A photograph of MMIPs suspended in water in the absence (left image) and in the presence (right) of an externally placed magnet. [Color figure can be viewed in the online issue, which is available at wileyonlinelibrary.com.]

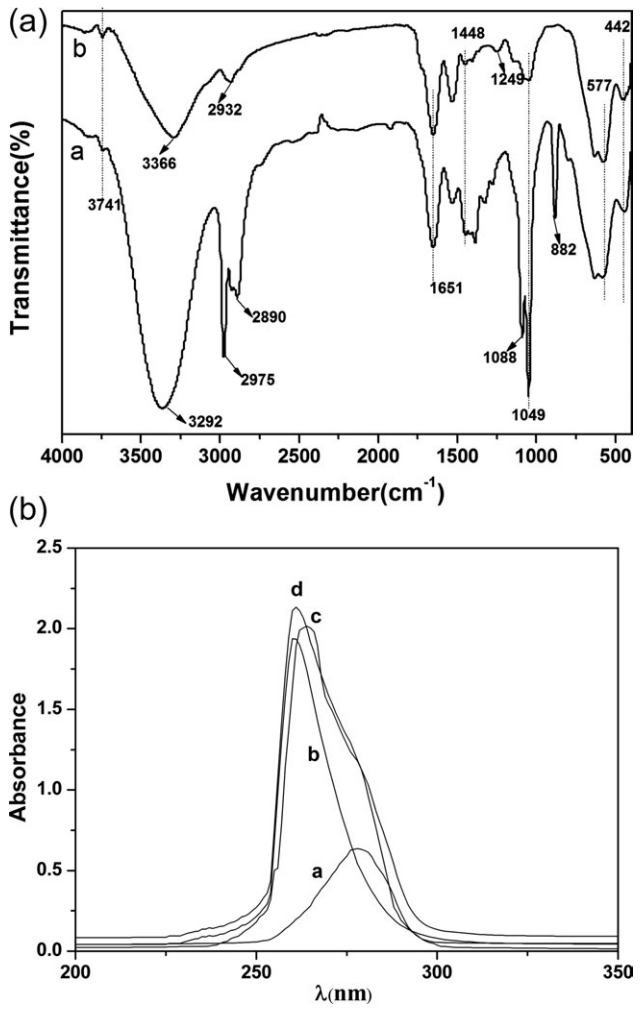

Figure 4. (a) FT-IR spectrum of the MNIPs (i) and MMIPs (ii). (b) UV absorption spectra of the mixture of PPs and MAA in DMSO solution. (i) PPs in DMSO solution (0.1 mmol/L); (ii) MAA in DMSO solution(4 mmol/L); (iii) the mixture of PPs and MAA in DMSO solution; (iv) theoretical sum of curves a and b.

collinear with the magnetic field, the Ms values of two materials were lower than that of the theoretical value for magnetite, which was 92 emu/g.[23,24] Moreover, the results from Figure 3(b) strongly suggested that the remained magnetic force in MMIPs could be attracted by an external magnetic field effectively. The results also demonstrated that MMIPs was a feasible magnetic separation carrier. The property has vital significance for the following batch mode experiments and recovery of material in the futher studies.

The infrared spectra of the MNIPs (a) and MNIPs (b) were measured and are shown in Figure 4(a), respectively. The main functional groups of the predicted structure can be observed with corresponding infrared absorption peaks. The peaks at 3741 cm^{-1} of MMIPs and MNIPs were attributed to the stretching vibrations of inner-surface O—H group. The absorption bands at 1651 cm^{-1} in the spectrum of MMIPs and MNIPs could be assigned to the C=O stretching vibration of ester (EGDMA). For MMIPs and MNIPs, additional vibrational bands at around 1448 cm^{-1} could be assigned to the covalently bound(C—H bending vibration). The absorption bands at 577 and 442 cm^{-1} of MMIPs and MNIPs corresponded to the Fe—O bond for Fe_3O_4 particles.[25] Moreover, MMIPs showed the strong additional bands at around 1249 cm^{-1}, which were assigned to the C—O symmetric stretching vibration of ester (EGDMA).[26] The peaks at 2932 cm^{-1} of MMIPs, 2975 cm^{-1} and 2890 cm^{-1} of MNIPs, indicated the presence of C—H stretching bands of —CH_3 and —CH_2 groups. The absorption band at 3366 cm^{-1} of the MMIPs and 3292 cm^{-1} of the MNIPs could be attributed to the stretching vibration of O—H bonds from MAA molecules. The paper also utilized UV–vis 765 spectrophotometer to investigate the reaction between the template molecule and the functional monomer. Figure 4(b) shows the UV absorption spectra of the PPs (i), MAA (ii), the mixture of PPs and MAA (iii) and theoretical sum of PPs and MAA in DMSO solution. From the Figure 4(b), we learned that the curve (iii) did not coincide with curve (iv). The actual absorbance of the mixture was less than the theoretical value of PPs and MAA in DMSO solution, and the maximum absorptive peak shifted slightly, which obviously explained that strong mutual reaction existed between PPs and MAA. All the results confirmed that the copolymerization of MAA and EGDMA has been initiated on the surface of M@Y in the presence of AIBN.

Figure 5 shows the TGA of the MMIPs and MNIPs. As shown in Figure 5, the first weight loss stage around 100°C can be ascribed to the evaporation of water molecules for each particle, which was 4.17 and 3.64% for MMIPs and MNIPs, respectively.[27] The second weight loss stage started at 500°C for MMIPs and MNIPs, respectively. In this stage, the mass loss of the MMIPs was more than MNIPs attributed to thicker imprinted film of MMIPs were 31.89 and 26.79%, respectively. Even more, the last weight loss stage occured at 800°C, there were significant differences of the mass loss of yeast for MMIPs and MNIPs, 17.22 and 10.75%, respectively. Compared with MMIPs and MNIPs, the remaining mass for MMIPs and MNIPs were attributed to the thermal resistance of magnetite nanoparticles, and the quantity of Fe_3O_4 hollow microspheres in the MMIPs and MNIPs was 46.72 and 59%, respectively.

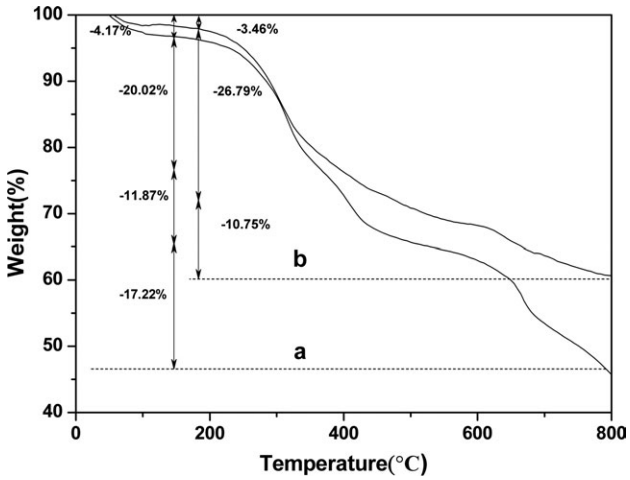

Figure 5. TGA of the MMIPs (a) and MNIPs (b).

Table I. Adsorption Selectivity of MMIPs and MNIPs in a Simulated Effluent

	MMIPs			MNIPs			
Pyrethroid pesticides	C_e (mg/L)	K_d (L/g)	k	C_e (mg/L)	K_d (L/g)	k	k'
Beta-cypermethrin	31.91	1.014		38.14	0.195		
Beta-cyfluthrin	36.59	0.373	2.718	37.93	0.218	0.894	3.04
Coexisting	34.04	0.700	1.449	38.02	0.208	0.938	1.54

Elemental analysis was used to ascertain each modification. The results are shown in Table I. After copolymerization, carbon and hydrogen composition were increased. The increase was attributed to the formation of organic polymer coating. It could also be found that the elemental compositions of the MMIPs were different from that of the MNIPs, the carbon element were 21.62 and 19% for MMIPs and MNIPs especially, indicating the PP_{321} molecules were not able to completely leach from the MMIPs. According to the results, 4.32% of the template PPs (19.92 mg of PP_{321} on every gram of the MMIPs) was remained on the packing after washing of the MMIPs.

Effect of pH for Adsorption Medium

Optimization of pH value for adsorption medium plays a vital role in the adsorption studies. The pH of the solution affects the degree of hydrolyzation and speciation of PP_{321}, leading to a change in adsorption equilibrium and kinetics characteristics subsequently. The effect of pH on the adsorption of PP_{321} and the effect of initial pH on final pH are shown in Figure 6. It was observed that adsorption capacity of MMIPs and MNIPs was approximately constant over the pH range of 2.0–6.0, and then declined in the pH range of 6.0–9.0 as PP_{321} slowly be hydrolyzed and becomed epimerism [Figure 6(a)]. Moreover, adsorption of PP_{321} at low pH 2.0–6.0 did not cause significant change in pH [Figure 6(b)], indicating greater adsorption capacity at this pH range may be induced by the stability of PP_{321}. Thus, 5.0 as optimization of pH for the adsorption medium was selected in the following studies; and, the initial pH had the same effects for MMIPs and MNIPs, but the adsorption capacity strongly indicated the imprinting effect.

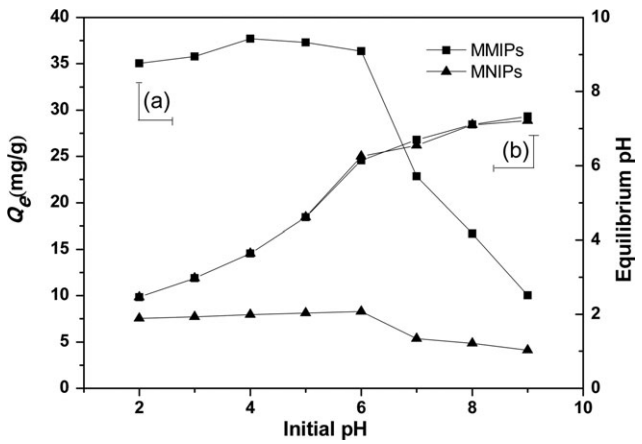

Figure 6. (a) Effect of pH on adsorptive removal of PP_{321}. (b) Effect of initial pH on equilibrium pH.

Adsorption Isotherms

The binding properties of MMIPs and MNIPs for PP_{321} were studied by the static equilibrium adsorption, and then the equilibrium data were fitted to the Langmuir[28] and Freundlich[29] isotherm models.

Moreover, comparison of Langmuir and Freundlich isotherm models for PP_{321} adsorption onto MMIPs and MNIPs, nonlinear regression are also illustrated in Figure 7. As shown in Figure 7, when the equilibrium concentration increased, the equilibrium adsorption capacity (Q_e) for PP_{321} first increased sharply. After a time, it was increased slowly, and finally attained to the maximum point as expected. The maximum adsorption capacity for MMIPs and MNIPs was 39.64 and 10.28 mg/g at 298 K, respectively. The values illustrated the good specificity for the imprinted molecule. By fitting the experimental data with Langmuir and Freundlich isotherm equations, it was also found that the Langmuir isotherm model was just a little better than the Freundlich model to fit the equilibrium data, attributed to a relatively smaller concentrate range of PP_{321}.

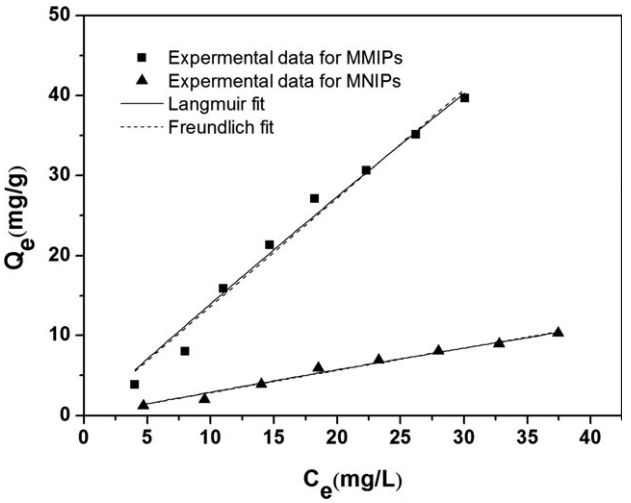

Figure 7. Adsorption isotherms of MMIPs and MNIPs.

Table II. Elemental Composition of the Particles from Elemental Analysis

Particle type	C (%)	H (%)	N (%)
MNIPs	19.00	2.742	2.681
MMIPs	21.62	3.199	2.671

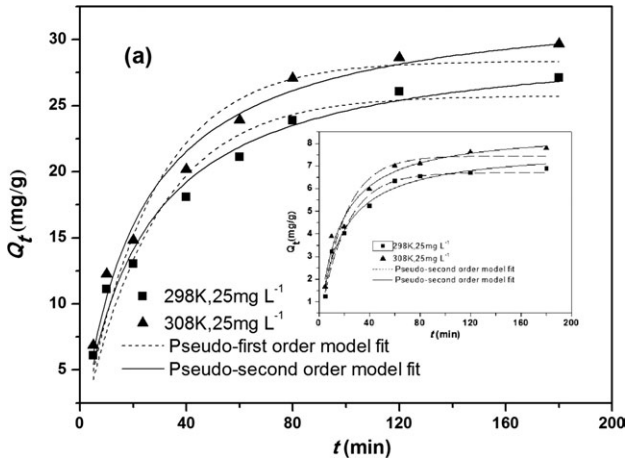

Figure 8. Pseudo-second-order rate equation for PP_{321} adsorption onto MMIPs (a) and MNIPs (b) using nonlinear regression.

Adsorption Kinetics

The kinetic data obtained were analyzed by using pseudo-first-order rate equation[30] and pseudo-second-order rate equation.[31]

The adsorption rate constants and linear regression values from the two rate equations are summarized in Table II. And the pseudo-second-order rate equation for PP_{321} adsorption onto MMIPs and MNIPs, nonlinear regression is shown in Figure 8. On the basis of the pseudo-second-order model, the initial adsorption rate (h, g/mg min) and half-equilibrium time ($t_{1/2}$, min) are also listed in Table II according to the following equations:[32]

From the favorable fit between experimental and calculated values of Q_e (R^2 values above 0.97), it could be demonstrated that the adsorption of PP_{321} followed pseudo-second-order kinetics well; and, it was assumed that the chemical process could be the rate-limiting step in the adsorption process for PP_{321}.[33] From Figure 8, pseudo-second-order kinetics lines deviated substantially from the experimental points around the first 40 min. The observed deviation from experimental data could be attributed to the sharp fall in concentration gradient, after the initial rapid adsorption of PP_{321} molecules onto the large amount of vacant binding sites.[34] During this time, it was believed that there was a switch between mass transfer diffusion control and pore diffusion control. A change in adsorption mechanism may have occurred after the first 40 min for PP_{321} adsorption.[35]

Selectivity Analysis of the MMIPs

To measure the selective recognition of PP_{321}, the recognition of competitive PPs was studied. During the experiment, 10 mL of the single PPs solution contained 0.4 mg was prepared, respectively. Meantime, 10 mL of the coexisting PPs solution (PP_{321}, beta-cyfluthrin) in which each pesticides contained 0.2 mg was also provided. Then, the aforementioned solution was treated according to the procedure of batch mode binding studies under optimal conditions. And the concentration of each pesticide in the solvent phase was determined with UV–vis 765 spectrophotometer (set wavelength at 278, 275, and 276 nm for PP_{321}, beta-cyfluthrin, coexisting solution, respectively).

The distribution coefficients (K_d), selectivity coefficients (k), and relative selectivity coefficient (k') of beta-cyfluthrin with respect to PP_{321} can be obtained according to eqs. (1–3).[26]

$$K_d = Q_e/C_e \tag{1}$$

$$k = K_{d(PP_{321})}/K_{d_{(X)}} \tag{2}$$

$$k' = k_M/k_N \tag{3}$$

X is the competitive PPs. K_M and K_N are the selectivity coefficients of MMIPs and MNIPs, respectively. Values of K_d, k, and k' are summarized in Table III. From the data in Table III, the K_d values of MMIPs were greater than those of MNIPs, showing that MMIPs had a large amount of sites on the surface. k indicated that MMIPs possessed the highest molecular recognition selectivity to PP_{321} among competitive PPs. k' expressed the adsorption affinity of recognition sites on MMIPs and MNIPs to the template molecules. The value of k' was 3.04 and 1.54 for beta-cyfluthrin and the coexisting PPs solution, indicating that the selectivity of MMIPs was more than MNIPs. And the recognition for competitive PPs was that PP_{321} was superior to beta-cyfluthrin. The results suggested that the imprinting process significantly improved adsorption selectivity to the imprinted template.

CONCLUSIONS

In this study, attachment of magnetic nanoparticles to yeast via robust linkages was achieved by co-precipitation reaction of $FeCl_3{\cdot}6H_2O$ and $FeCl_2{\cdot}4H_2O$. Then, we developed an efficient method for synthesis of magnetic surface molecular imprinting polymers using magnetic yeast particles as solid-support. The prepared MMIPs exhibited uniform morphology, favorable saturation magnetization, thermal stability, and excellent specific

Table III. Kinetic Constants for the Pseudo-First-Order Equation and Pseudo-Second-Order Equation

			Pseudo-first-order equation				Pseudo-second-order equation				
Sample	C_o (mg /L)	T (K)	$Q_{e,exp}$ (mg/g)	$Q_{e,c}$ (mg/g)	k_1 (L/min)	R^2	$Q_{e,c}$ (mg/g)	$k_2 \times 10^{-3}$ (g/mg min)	H (mg/g min)	$t_{1/2}$ (min)	R^2
MMIPs	25	298	27.12	25.73	0.0364	0.9357	30.26	1.440	1.320	22.95	0.9773
	25	308	29.67	28.36	0.0382	0.9447	33.24	1.380	1.520	21.80	0.9807
MNIPs	25	298	6.890	6.700	0.0481	0.9685	7.780	7.370	0.450	17.44	0.9743
	25	308	7.790	7.440	0.0501	0.9487	8.590	7.110	0.520	16.37	0.9738

recognition. Pan et al. have synthesized MIPs based on magnetic halloysite nanotubes composites to selectively adsorb 2,4,6-trichlorophenol, the MMIPs exhibited magnetic property (Ms = 2.74 emu/g). However, MMIPs prepared in our research exhibited higher magnetic property (Ms = 17.87 emu/g). Adsorption isotherms and kinetics prove that it is efficient to adsorb PP321 from the experimental water samples and to separate adsorbent easily by an external magnetic field, indicating a significant selective adsorption of trace PP_{321} from PP**s**-contaminated wastewater. We believe that these surface imprinted polymers with magnetite composites as supports can be one of the most promising candidates for environmental pollutants separation.

ACKNOWLEDGMENTS

This work was financially supported by Ph.D. Programs Foundation of Ministry of Education of China No. 20110205110014.

REFERENCES

1. Hassell, K. A. The Biochemistry and Uses of Pesticides; VCH, Weinheim: Germany, **1990**; p 174.
2. Davis, J. H. In The Pyrethroid Insecticides; Leahey, J. P., Ed.; London, **1985**; p 1.
3. Elliott, M. In Synthetic Pyrethroids; Symposium Series *42*; Elliott, M. Ed.; American Chemical Society: Washington, DC, **1977**; p 1.
4. Fan, J. L.; Zhang, J.; Zhang, C. L.; Ren, L.; Shi, Q. Q. *Desalination.* **2011**, *267*, 139.
5. Spinosa, H. D. S.; Silva,Y. M.; Nicolau, A. A.; Bernardi, M. M.; Lucisano, A. *Physiol. Behav.* **1999**, *67*, 611.
6. Sharif, Z.; Man, Y. B. C.; Hamid, N. S. A.; Keat, C.C. *J. Chromatogr. A.* **2006**, *1127*, 254.
7. Wang, B.; Wang, R. M. *Chem. Res. Appl.* **2010**, *2*, 129.
8. Gao, B. J.; Lu, J. H.; Chen, Z. P.; Guo, J. F. *Polymer.* **2009**, *50*, 3275.
9. Gao, B. J.; Wang, J.; An, F. Q.; Liu, Q. *Polymer.* **2008**, *49*, 1230.
10. Pan, J. M.; Zou, X. H.; Yan,Y. S.; Wang, X.; Guan, W.; Liu, Y. *Appl. Clay. Sci.* **2010**, *50*, 260
11. Lee, S. W.; Yang, D. H.; Kunitake, T. *Sen. Actuators, B.* **2005**, *104*, 35.
12. Zhou,W. H.; Lu, C. H.; Guo, X. C.; Chen, F. R.; Yang, H. H.; Wang. X. R. *J. Mater. Chem.* **2010**, *20*, 880.
13. Zhang, Z. H.; Zhang, H. B.; Hua, Y. F.; Yao, S. Z. *Ana. Chim. Acta.* **2010**, *661*, 173.
14. Sağ, Y.; Akçael, B.; Kutsal. T. *Process Biochem.* **2001**, *37*, 35.
15. Chojnacka, K.; Chojnacki, A.; Górecka. H. *Chemosphere.* **2005**, *59*, 75.
16. Pagnanelli, F.; Esposito, A.; Toro, L.; Vegliò, F. *Water Res.* **2003**, *37*, 627.
17. Bai, B.; Wang, P. P.; Wu, L.; Yang, L.; Chen, Z. H. *Mater. Chem. Phys.* **2009**, *114*, 26.
18. Jing, T.; Du, H. R.; Dai, Q.; Xia, H.; Niu, J. W.; Hao, Q. L.; Mei, S. R.; Zhou, Y. K. *Biosens. Bioelectron.* **2010**, *26*, 301.
19. Pan, J. M.; Xu, L. C.; Dai, J. D. *Chem. Eng. J.* **2011**, *174*, 68.
20. Chen, L. G.; Zhang, X. P.; Sun, L.; Xu, Y.; Zeng, Q. L.; Wang, H.; Xu, H. Y.; Yu, A. M.; Zhang, H. Q.; Ding, L. *J. Agric. Food Chem.* **2009**, *57*, 10073.
21. Kale, S. S.; Lokhande, C. D. *J. Mater. Chem. Phy.* **2000**, *62*, 103.
22. Wang, X.; Wang, L. Y.; He, X. W.; Zhang, Y. K.; Chen, L. X. *Talanta.* **2009**, *78*, 327.
23. Zaitsev, V. S.; Filimonov, D. S.; Presnyakov, I. A.; Gambino, R. J.; Chu, B. J. *Colloid Interface Sci.* **1999**, *212*, 49.
24. Kodama, R. H.; Berkowitz, A. E. J.; Mcniff, E. J.; Foner, S. *Phys. Rev. Lett.* **1996**, *77*, 394.
25. Kim, I. T.; Nunnery, G. A.; Jacob, K.; Schwartz, J.; Liu, X. T.; Tannenbaum, R. J. *Phys. Chem. C.* **2010**, *114*, 6944.
26. Pan, J. M.; Yao, H.; Xu, L. C.; Ou, H. X.; Huo, P. W.; Li, X. X.; Yan, Y. S. *J. Phys. Chem. C.* **2011**, *115*, 5440.
27. Feng, B.; Hong, R. Y.; Wang, L. S.; Guo, L.; Li, H. Z.; Ding, J.; Zheng, Y.; Wei, D. G. *Colloids Surf. A.* **2008**, *328*, 52.
28. Mazzotti, M. J. *Chromatogr. A.* **2006**, *1126*, 311.
29. Allen, S. J.; Mckay, G.; Porter, J. F. *J. Colloid Interface Sci.* **2004**, *280*, 322.
30. Ho, Y. S.; McKay, G. *Water Res.* **1999**, *33*, 578.
31. Ho, Y. S.; McKay, G. *Process Biochem.* **1999**, *34*, 451.
32. Wu, Z. J.; Joo, H.; Lee, K. *Chem. Eng. J.* **2005**, *11*, 227.
33. Baydemir, G.; Andac, M.; Bereli, N.; Say, R.; Denizli, A. *Chem. Res.* **2007**, *46*, 2843.
34. Ofomaja, A. E. *Chem. Eng. J.* **2008**, *143*, 85.
35. Ofomaja, A. E. *Bioresour. Technol.* **2010**, *101*, 5868.